nature COMMUNICATIONS

ARTICLE

Received 12 Jul 2012 | Accepted 24 Jan 2013 | Published 5 Mar 2013

DOI: 10.1038/ncomms2542 OPEN

The interaction between OsMADS57 and OsTB1 modulates rice tillering via *DWARF14*

Siyi Guo[1,2,*], Yunyuan Xu[1,*], Huanhuan Liu[1,2], Zhiwei Mao[1], Cui Zhang[1], Yan Ma[1], Qirui Zhang[1], Zheng Meng[1] & Kang Chong[1,3]

Rice tillering is a multigenic trait that influences grain yield, but its regulation molecular module is poorly understood. Here we report that OsMADS57 interacts with OsTB1 (TEOSINTE BRANCHED1) and targets *D14* (*Dwarf14*) to control the outgrowth of axillary buds in rice. An activation-tagged mutant *osmads57-1* and *OsMADS57*-overexpression lines showed increased tillers, whereas *OsMADS57* antisense lines had fewer tillers. *OsMIR444a*-overexpressing lines exhibited suppressed *OsMADS57* expression and tillering. Furthermore, *osmads57-1* was insensitive to strigolactone treatment to inhibit axillary bud outgrowth, and *OsMADS57*'s function in tillering was dependent on *D14*. *D14* expression was downregulated in *osmads57-1*, but upregulated in antisense and *OsMIR444a*-overexpressing lines. OsMADS57 bound to the CArG motif [C(A/T)TTAAAAAG] in the promoter and directly suppressed *D14* expression. Interaction of OsMADS57 with OsTB1 reduced OsMADS57 inhibition of *D14* transcription. Therefore, *OsMIR444a*-regulated *OsMADS57*, together with *OsTB1*, target *D14* to control tillering. This regulation mechanism could have important application in rice molecular breeding programs focused on high grain yield.

[1] The Key Laboratory of Plant Molecular Physiology, Institute of Botany, Chinese Academy of Sciences, Beijing 100093, China. [2] University of Chinese Academy of Sciences, Beijing 100049, China. [3] National Center for Plant Gene Research, Beijing 100093, China. * These authors contributed equally to this work. Correspondence and requests for materials should be addressed to K.C. (email: chongk@ibcas.ac.cn).

Transcription factors of the MADS-domain family (named for yeast MCM1, plant AGAMOUS and DEFICIENS, and mammal Serum Response Factor) are highly conserved among fungi, animals and plants. Genetic interactions of MADS-box family members are involved in flowering, floral organ identity and development, embryogenesis and meristem differentiation. In rice, the genetic interactions among the four AG subfamily members, *OsMADS3*, *OsMADS13*, *OsMADS21* and *OsMADS58*, determine the identity of floral organs[1]. *OsMADS6* interacts with *SUPERWOMAN1*, *OsMADS3, OsMADS58*, *OsMADS13* and *DROOPING LEAF* to control floral organ identities and meristem fates[2]. At the protein level, MADS proteins generally interact with themselves or other proteins to form homodimer or heterodimer for performing their functions[3–5]. MADS-domain proteins recognize and bind to specific palindromic DNA sequences with a CArG core consensus element to regulate the expression of target genes[4,6–8]. The 'floral quartet model' suggests that floral organ identity regulators of the MADS-box family assemble into organ-specific quaternary transcription factor complexes to control the identity and development of floral organs. However, less is known about how the transcription factors and their targets function *in planta*.

With regard to spatial expression patterns of *MADS* genes, it is worth noting that several genes in the MIKC^c-type group (MEF-like (M-), intervening (I-), Keratin-like (K-) and C-terminal (C-) domains), the *AGL12*-like clade, the *STMADS11*-like clade and the *AGL17*-like clade are predominantly expressed in vegetative tissues. In rice, *AGL17*-like clade genes, including *OsMADS23*, *OsMADS25*, *OsMADS27*, *OsMADS61* and *OsMADS57* (ref. 9) exhibit this pattern and are expressed predominantly in vegetative tissues. This implies a unique function in vegetative development[9,10]. However, the specific mechanism of MADS protein interaction with target genes for the induction of function in vegetative organ development is poorly understood. *MADS* and *TCP* (*TEOSINTE BRANCHED1* (*TB1*) from maize, *CYCLOIDEA* from *Antirrhinum* and *PROLIFERATING CELL FACTOR* from rice) have been shown to cofunction in determining meristem identity and control organ morphogenesis[11]. In floral organogenesis, *MADS* genes primarily mediate organ identity, while *TCP* genes regulate floral meristem symmetry. *TCP* genes also participated in the regulation of vegetative branching patterns[12–14]. *TB1* was under strong selection as maize became an agricultural cultivar, and has been shown to function as a reducer of axillary bud growth in maize, rice and Arabidopsis[12,13,15]. The expression of *AGL17*-like clade genes in vegetative tissues hints that they may also have a role in the differentiation of axillary buds. However, there is currently no evidence to support this supposition, and it remains unclear how TCP and MADS coordinate the regulation of branching in plants.

Tillering or branching genes function during the initiation of morphogenesis and/or the outgrowth of axillary buds. A series of shoot-branching mutants have been identified in diverse plant species, including *max* (*more axillary growth*) in Arabidopsis, *rms* (*ramosous*) in pea, *dad* (*decreased apical dominance*) in petunia, *tb1* in maize and *dwarf* (*d*) in rice[12,15–20]. The rice mutant *moc1* (*monoculm 1*) has characteristic monoculms, lacking any tillers. The transcription factor MOC1, together with MIP1, controls the initiation and outgrowth of axillary buds in rice[21]. Degradation of MOC1 with APC/C$^{TAD1/TE}$ in a cell-cycle-dependent manner mediates rice tillering[22,23]. In contrast to these genes that reduce tillering, there are a series of rice mutants that confer an increased number of tillers. These include *d3*, *d10*, *d17*, *d33*, *ostb1*, *d27* and *d14*, and their corresponding genes are suggested to be involved in the regulation of axillary bud outgrowth for tillering in rice. *D14* functions in strigolactone (SL) signalling to control tillering, while *D27* functions in SL biosynthesis [19,24,25]. Several components of the SL biosynthesis pathway, including carotenoid cleavage dioxygenase (CCD)7, CCD8, MORE AXILLARY GROWTH1 (MAX1) and D27, have been implicated in axillary bud outgrowth[16–19,26,27]. Expression of *D27* is directly regulated by GRAS transcription factors, NODULATION SIGNALLING PATHWAY1 (NSP1) and NSP2 in *Medicago truncatula* and rice[28]. Genetic and biochemical studies suggest that D14/D88/HTD2 functions in SL biosynthesis or signal transduction, and that MAX2/D3/RMS4 and DAD2/D14 perceive and transduce the signals[20,24,25]. However, it remains unclear how such genes are directly coordinated to function in axillary bud outgrowth in plants. Here we explore the role of *OsMADS57* in the regulation of tillering using transgenic lines and related mutants. Our results show that *OsMADS57* is negatively regulated by miR444a, and that OsMADS57 subsequently negatively regulates the expression of *D14*, thereby affecting tillering. This negative regulation by OsMADS57 is suppressed by interaction with OsTB1, leading to the balanced expression of D14 for tillering.

Results

The *osmads57-1* mutant has increased tillering. *OsMADS57* was predicted to encode a protein containing a MADS-box domain, a variable I region, a conserved K-box domain and a C-terminal region (Fig. 1a). Phylogenetic analysis grouped OsMADS57 into the *AGL17*-like lineage (Fig. 1c) that is predominantly expressed in vegetative tissues[9,29]. The T-DNA insertion mutant line PFG_3A-05432.L, named henceforth as *osmads57-1*, was obtained from RiceGE, the Rice Functional Genomics Express Database of Korea[30]. The T-DNA was inserted into P0617A09 at the 86,816-bp position in the rice genome, where the predicted gene *OsMADS57* is annotated. DNA gel blot analysis showed one copy of the T-DNA in the genome (Supplementary Fig. S1b). The gene contains eight exons and seven introns and is 6,094 bp in total length (Fig. 1b). The T-DNA insertion position is 5,275 bp from the transcriptional initiation site in *OsMADS57* (Fig. 1b and Supplementary Fig. S1a).

The T-DNA insertion caused a fused open reading frame of 675 bp in *osmads57-1*, rather than the original 726 bp open reading frame of *OsMADS57* in wild type (WT; Fig. 1b and Supplementary Fig. S1c,d). In the mutant, 24 amino-acid residues at the OsMADS57 C terminus were replaced with a peptide of 7 amino-acid residues encoded by the T-DNA to form a fusion protein, OsMADS57F (Supplementary Fig. S1a). OsMADS57F was predicted to contain the MADS-box domain, the I region and the K-box domain, but not the intact C terminus (Fig. 1a). The transcription level of a 5′-fragment of *OsMADS57* was increased in the mutant, but a 3′-fragment was dramatically decreased (Fig. 1d). Therefore, *osmads57-1* is a T-DNA insertion mutant that overexpresses the truncated OsMADS57.

Unlike the other known *MADS* genes rice mutants, *osmads57-1* did not have any significant alterations in floral organogenesis or development, except for crooked anthers and altered primary root growth compared with WT plants (Supplementary Fig. S2). Primary root growth was repressed in the *osmads57-1* mutant compared with WT plants until 7 days after germination (DAG; Supplementary Fig. S2a,b). This significant difference disappeared after 14 days. The *osmads57-1* mutant showed an obvious increase in the number of tillers from the 4th-leaf stage to the mature stage (Fig. 1e,f). Histological analysis revealed the appearance of outgrowth of axillary buds as early as 7 DAG in *osmads57-1*, whereas this outgrowth was absent in WT Dongjin (DJ) (Fig. 1g). At day 15, *osmads57-1* plants showed two axillary bud outgrowths, whereas WT showed only one. Therefore, enhanced expression of truncated OsMADS57 may cause accelerated emergence of axillary bud outgrowth in *osmads57-1* plants.

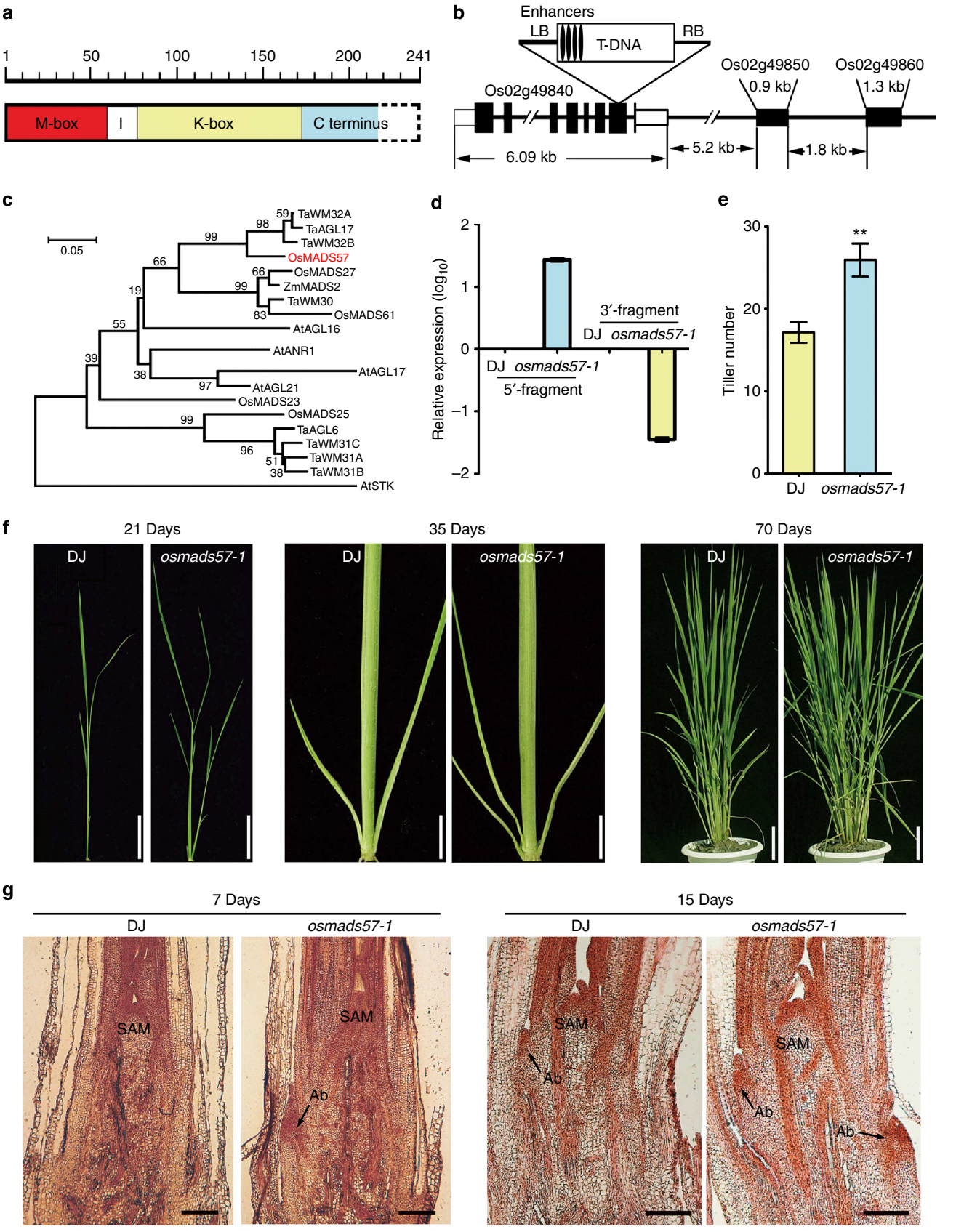

Figure 1 | *OsMADS57* structure and phenotype of the *osmads57-1*. (**a**) OsMADS57 sketch; MEF-like (M-box); intervening (I); Keratin-like (K-box); Carbon (C)-terminus domains; Dashes-box, the truncated-part; Scale numbers, amino-acid residues. (**b**) T-DNA insertion in *OsMADS57* (Os02g49480). (**c**) Phylogenetic tree of *AGAMOUS*-like*17* genes. (**d**) Transcript patterns in *osmads57-1* at 15 DAG. (**e**) Tiller numbers at 70 DAG. Values represent means ± s.e. of ten plants. $^{**}P < 0.01$ by Student's *t*-test. (**f**) Tillering phenotypes in various stages. Scale bar, 5 cm. (**g**) Longitudinal sections of shoot meristems (SAM) and axillary buds (Ab). Scale bars, 100 μm.

OsMADS57 and OsMIR444a are involved in axillary bud development. To confirm the phenotypes further, we created six *OsMADS57*-overexpression lines (OE) and three antisense transgenic lines (AS). Quantitative reverse transcription–PCR (qRT–PCR) assays revealed that *OsMADS57* expression was enhanced in OE lines (for example, OE1) and suppressed in antisense lines (for example, AS3) compared with WT plants (Fig. 2a,c). Antisense line AS3 had fewer tillers than WT Zhonghua10 (ZH10). In contrast, the OE1 line had more tillers than ZH10 (Fig. 2a,e), without alteration in floral organogenesis (Supplementary Fig. S2c). Therefore, *osmads57-1* is likely a gain-of-function mutant.

OsMADS57 was predicted to be a target of the 21-nt non-coding RNA miR444a (Fig. 2b), which is conserved in monocots such as wheat, barley, maize, sorghum and sugarcane[31]. We created *OsMIR444a*-overexpressing rice lines (miROE; Supplementary Fig. S3), and qRT–PCR and RNA gel blot analyses indicated that *miR444a* transcript levels were increased in these lines compared with WT (Fig. 2d and Supplementary Fig. S4). Correspondingly, *OsMADS57* expression was significantly reduced in the miROE lines (Fig. 2c). The miROE lines had fewer tillers than did WT, similar to the AS lines (Fig. 2a,e). By contrast, tiller numbers in the miROE lines were altered significantly compared with *osmads57-1* (Fig. 1e,f) and OE lines (Fig. 2a,e). The miROE lines were similar to WT ZH10 in root development and floral organogenesis and development (Supplementary Fig. S2a,c). These results demonstrate that the expression of *OsMADS57* is repressed by *OsMIR444a* to control tillering.

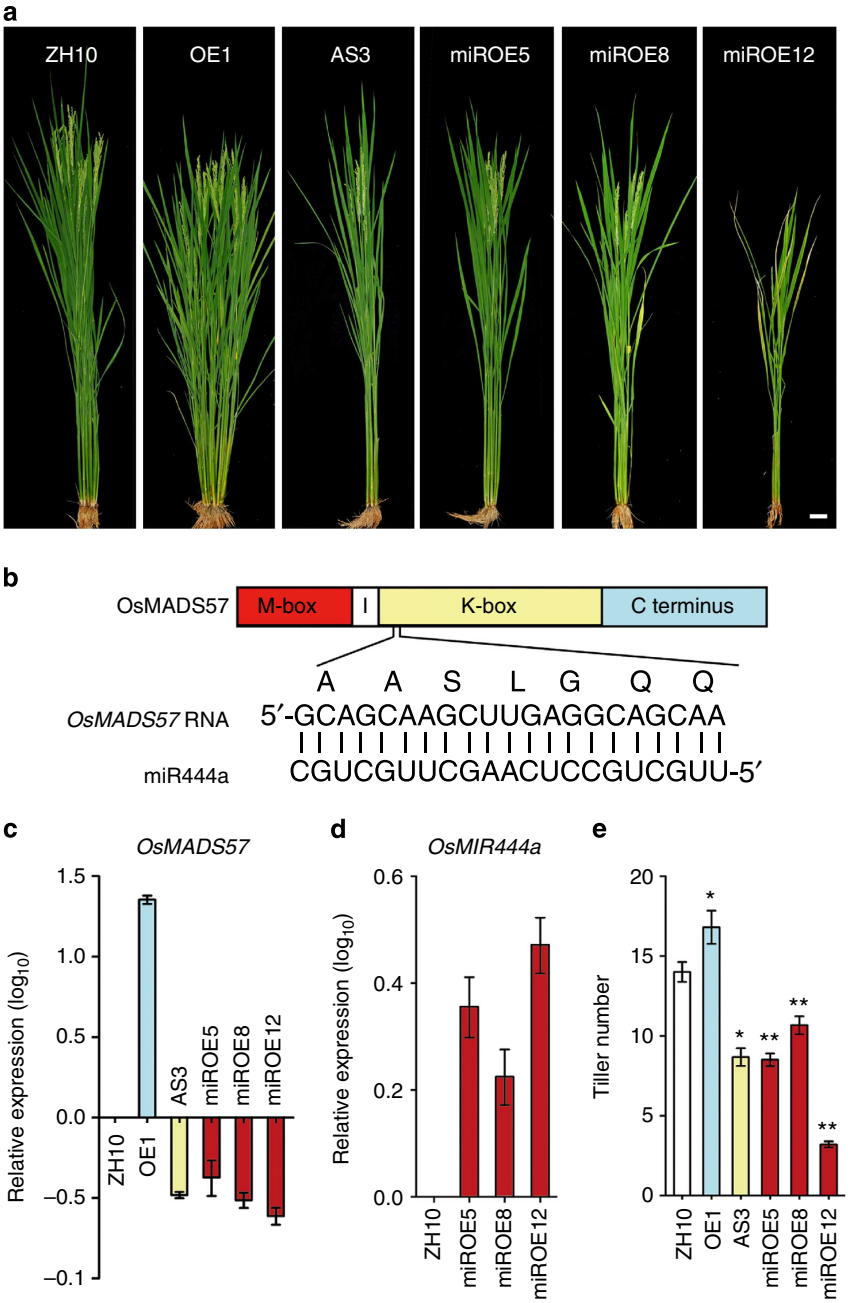

Figure 2 | Morphological comparison of the transgenic lines. (**a**) Tillering phenotypes. Scale bar, 5 cm. (**b**) miR444a and its target sequence sketch. (**c**,**d**) Relative expression in the transgenic lines. (**e**) Tiller numbers at 70 DAG. Values represent means ± s.e. of ten plants. $^{*}P<0.05$, $^{**}P<0.01$ by Student's *t*-test.

Expression patterns of OsMADS57 and its repressor activity. We searched the Genevestigator database, the HANADB-Os database and the eFP browser of rice microarray data[9,32,33] for *OsMADS57* expression data. The results indicated that *OsMADS57* expression was higher during tillering and stem-elongation stages than other stages in rice (Supplementary Fig. S5a). It was highly expressed in leaf tissues and weakly expressed in other organs (Supplementary Fig. S5b–d). Quantitative RT–PCR assays showed that the highest transcript level of *OsMADS57* was in sheaths and leaves, and that no signals were observed in the culm (Fig. 3a). On the other hand, expression of miR444a was found in all organs except for roots. RNA *in situ* hybridization assays revealed *OsMADS57* expression predominantly in shoot apical meristems and axillary buds (Fig. 3b). This suggests that *OsMADS57* is involved in the outgrowth of axillary buds.

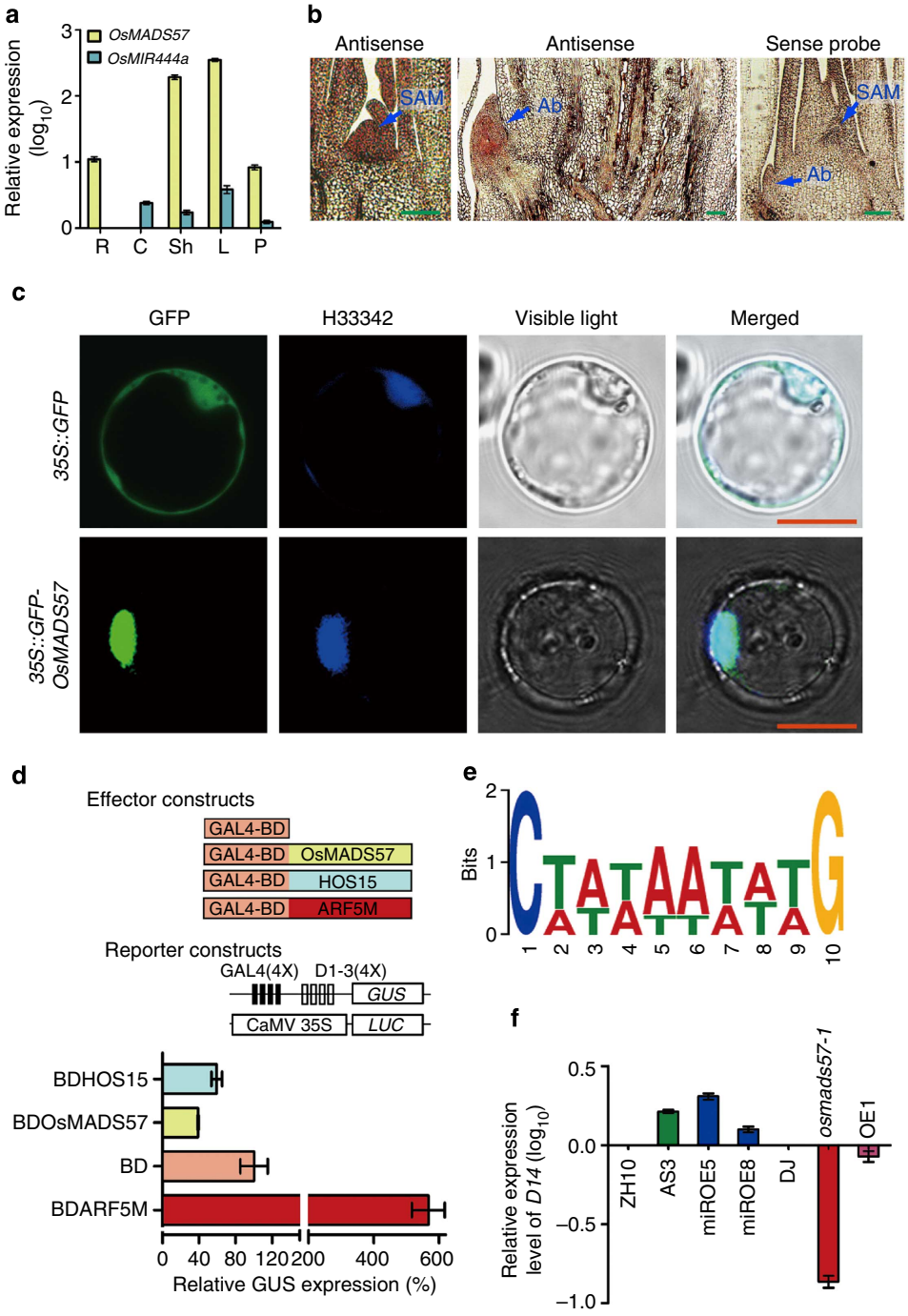

Figure 3 | Expression patterns of *OsMADS57* and its regulation activity. (**a**) Expression in roots (R), culms (C), sheaths (Sh), leaves (L) and panicles (P). (**b**) RNA *in situ* hybridization of *OsMADS57* in SAM and axillary buds (Ab). Scale bars, 100 μm. (**c**) Localization of GFP- OsMADS57 in rice protoplasts. H33342, a nuclear staining dye. Scale bars, 10 μm. (**d**) The transcriptional repression activity assays in Arabidopsis protoplasts. (4X)-D1-3(4X), four upstream GAL4 DNA-binding sites in the promoter of *GUS*; CaMV 35S, a promoter of *LUC* reporter (the internal control). HOS15, a transcription suppressor, and ARF5M, an activator, were used as the controls. (**e**) The preferred CArG-box binding motif for OsMADS57 from the expression level and frequency of the 97 regulated genes. (**f**) *D14* expression in various lines.

In subcellular localization assays, green fluorescent protein (GFP)-OsMADS57 fluorescence completely overlapped with H33342 nuclear staining in rice protoplasts (Fig. 3c). By contrast, GFP fluorescence of the transgenic control cells was localized in the plasma membrane and cytoplasm. To identify the physical interaction between the regulatory transcription factor OsMADS57 and its DNA targets, a yeast one-hybrid system was used (Fig. 3d). Transcriptional activity assays using protoplasts revealed that OsMADS57 fused to the DNA-binding domain from GAL4 (BD), and significantly repressed the expression (40%) of the target reporter gene *GUS*, which contained four GAL4 DNA-binding sites in the promoter, compared with BD alone (set to 100%). Meanwhile, for the previously reported repressed gene *HOS15* (ref. 34), which was used as a positive control for the repressor activity, *GUS* expression was 60% of that with BD alone. The negative control, ARF5M, activated *GUS* expression 5.8-fold compared with BD only. Therefore, OsMADS57 has the ability to repress transcription of its target genes.

Genome-wide gene expression analysis of OsMADS57. To investigate potential target genes of *OsMADS57*, we performed Affymetrix rice microarray assays using probes from *osmads57-1* and WT DJ (Supplementary Figs S6 and S7a). The signal value ($\log_2$ ratio) of *OsMADS57* was 2.99 in *osmads57-1*, which was similar to our qRT–PCR results (Fig. 1d and Supplementary Table S1). Microarray data analysis revealed that 175 genes upregulated and 19 genes downregulated by more than twofold ($|\log_2 \text{ ratio}| \geq 1$) in the *osmads57-1* mutant compared with DJ (Supplementary Fig. S7b and Table S1). GO analysis showed that transcription factor-, hormone-, cell division-, metabolism- and membrane-related genes were clustered in up- and down-regulated groups (Supplementary Table S2). Genes that have been demonstrated to promote tillering, such as *GA2ox4*, *GA2ox6* and *GA2ox9*, were found among the upregulated genes in the microarray data (Table 1)[18,35–38].

MADS-box transcription factors bind to the *cis*-element CArG box C(T/A)(T/A) (T/A)(T/A)(T/A)(T/A)(T/A)(T/A)G (refs 4,6,7,39). We performed *cis*-element screening in the region −1,500 to −1 bp from the initiation code for all 175 up- and 19 downregulated genes. Among all of the differentially regulated genes, which should include both direct and indirect targets, the CArG *cis*-element was identified in 86 upregulated genes and 11 downregulated genes (Supplementary Fig. S7b and Table S3). On the basis of MEME suite analysis of the expression level and frequency of the 97 regulated genes, we characterized the preferred CArG box of OsMADS57 (Fig. 3e). $C_1xxxxxxxxG_{10}$ was the strongest element contributing to the binding; other important contributors were the elements at $(A/T)_5$ and $(A/T)_6$, as well as $(T/A)_2$ (Fig. 3e). Importantly, the frequencies of the preferred CArG *cis*-element in random gene sequences from the whole genome were much lower than in the regulated genes (Supplementary Fig. S7c).

Using the potential OsMADS57-binding motif to search for further target sequences, one of the preferred CArG-box motifs [C(A/T)TTAAAAAG] was found in the promoter of *D14* (Os03g10620), which was previously identified as controlling tiller development[20,24,40]. In our Affymetrix GeneChip assay, unexpectedly, *D14* was not among the regulated genes, possibly because of biased probes for *D14* on the chip (Supplementary Fig. S8 and Table S3). We examined the expression of *D14* by qRT–PCR in lines with various levels of *OsMADS57* expression (Fig. 3f). *D14* transcription was dramatically downregulated in the *osmads57-1* mutant, and somewhat downregulated in the *OsMADS57* OE line. Conversely, *D14* expression was upregulated in the *OsMADS57* AS and miROE lines. This suggests that expression of *D14* is negatively regulated by OsMADS57 in rice.

***D14* is a direct target of OsMADS57**. Two likely OsMADS57-binding CArG-boxes sites, site 1 [CTTTAAAAAG] and site 2 [CATTAAAAAG], were found at −2,281 to −2,272 bp and −1,320 to −1,311 bp from the initiation of *D14*, respectively (Fig. 4a)[20]. Electrophoretic mobility shift assays (EMSAs) revealed that the labelled target of either site 1 or 2 bound to OsMADS57-GST was shifted to bigger in the molecular weight on the gel (lanes 4 and 6) as compared with the target alone (lanes 2 and 8), or the negative control (lanes 3 and 9; Fig. 4b). Additionally, addition of GST antiserum to the binding reactions resulted in two additional retarded bands with increased molecular weight at the top of the lanes (lanes 5 and 7; Fig. 4b). At the same time, there was a loss of one band in the small-molecular weight on lanes 4–7, respectively, compared the controls. A ChIP assay using OsMADS57 antibody showed that the regions 'I' and 'II' of the *D14* promoter, which included site 1 and site 2 CArG motifs, respectively, were enriched in *osmads57-1* compared with WT (Fig. 4c and Supplementary Fig. S9). By contrast, there were no differences for regions 'III' and 'IV' between *osmads57-1* and WT. Thus, OsMADS57 targeted both the CArG *cis*-elements, site 1 and site 2, that were present in *D14*.

The activities of OsMADS57 and an N-terminal peptide of 168 amino-acid residues (OsMADS57N) were analysed in yeast via expression of the reporter gene *LacZ* driven by the *D14* promoter-*Pcyc1* (*D14p*). The effectors contained the GAL4-activation domain. The strains with the full-length or truncated genes grew well and were blue compared with the control (Fig. 4d). By contrast, yeast cells with *OsMADS57*, but lacking the *D14* promoter, did not turn blue. Therefore, the truncated protein bound to the *D14* promoter in yeast, as did the full-length gene.

Table 1 | Genes of known function in tillering with altered expression patterns in the *osmads57-1* mutant based on the microarray data.

Probe ID	Locus ID	Change (log2)	Putative function	Known phenotypes	References
OsAffx.15093.1.S1_s_at	LOC_Os05g43880 (*GA2ox4*)	1.61	Gibberellin 2-β-dioxygenase, putative	Gain-of-function mutant of *GA2ox4* showed increased tillers	Lo *et al.*[35]
Os.54940.1.S1_at	LOC_Os04g44150 (*GA2ox6*)	2.85	Gibberellin 2-β-dioxygenase, putative	Gain-of-function mutant *GA2ox6* showed increased tillers	Lo *et al.*[35]
OsAffx.24682.1.S1_s_at	LOC_Os02g41954 (*GA2ox9*)	2.41	Gibberellin 2-β-dioxygenase, putative	Gain-of-function mutant *GA2ox9* showed increased tillers	Lo *et al.*[35]
Os.37454.1.S1_at	LOC_Os01g38580 (*D10*-like)	4.70	β-Carotene 9,10-dioxygenase, putative, expressed	Loss-of-function mutant *d10* showed increased tillers	Arite *et al.*[18]

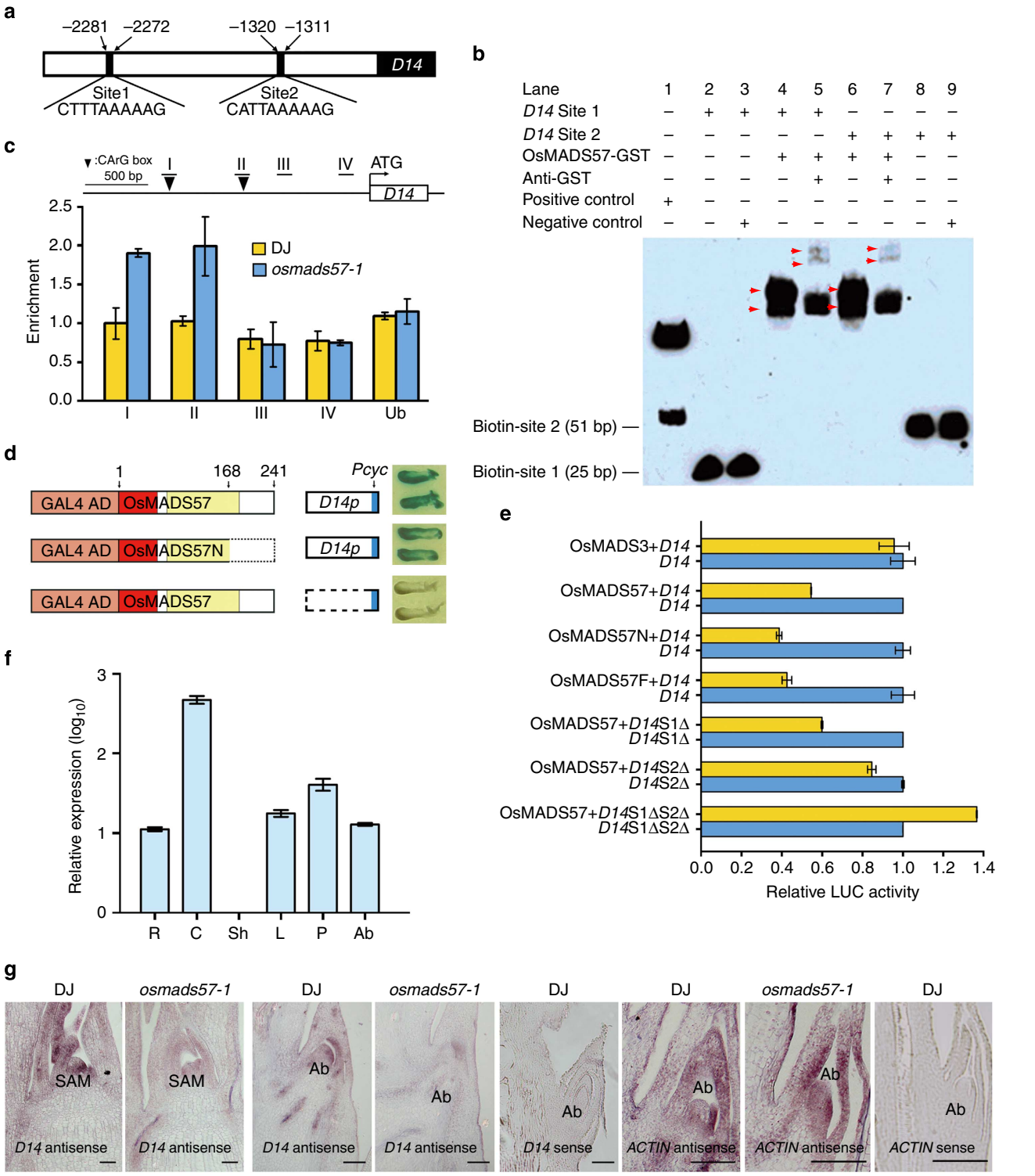

Figure 4 | OsMADS57 inhibits *D14* expression. (**a**) *D14* promoter sketch showing CArG-boxes. (**b**) EMSA of OsMADS57 binding the *cis*-elements. The amount of protein loaded in each lane was equal. (**c**) ChIP assay of 2-week-seedling to show OsMADS57-binding regions in *D14* promoter. Regions I and II contain the probes used in EMSA. The *UBIQUITIN* (Ub) promoter was used as a control. (**d**) Yeast one-hybrid analysis. The effectors contained the GAL4-activation domain. (**e**) Transcriptional repression activity assay in Arabidopsis protoplasts. S1Δ and/or S2Δ, deletion of site 1 and/or 2. (**f**) *D14* expression in roots (R), culms (C), sheaths (Sh), leaves (L), panicles (P) and axillary buds(Ab). (**g**) RNA *in situ* assay for *D14*. Scale bars, 100 μm.

A transcriptional regulation activity assay in protoplasts revealed that OsMADS57, OsMADS57N and the fusion protein OsMADS57F repressed the expression of the *D14* promoter driving the *luciferase* (*LUC*) reporter gene (Fig. 4e). On the other hand, the inhibition of OsMADS57 on *D14* was diminished by deleting the site 2 CArG box. When both binding sites were deleted from *D14*, OsMADS57 showed a increased *LUC* expression in the assay system (Fig. 4e). Therefore, OsMADS57 requires those sites to repress *D14* transcription.

Quantitative RT–PCR analyses revealed that *D14* expression was high in culms, but low in roots, leaves, panicles and axillary buds (Fig. 4f). RNA *in situ* hybridization demonstrated that *D14* transcripts were prominent at the shoot apical meristem (SAM) and axillary buds in WT, but were reduced in *osmads57-1* tissues (Fig. 4g). By contrast, *in situ* expression analysis of the *ACTIN* gene as a control showed no obvious difference between *osmads57-1* and WT. The expression pattern of *D14* overlapped with that of *OsMADS57* in the SAM and axillary buds (Fig. 3b). qRT–PCR assays revealed that the *D14* mRNA level was suppressed in *osmads57-1 in planta* (Fig. 3f). Therefore, OsMADS57 seems to target *D14* directly to suppress its transcription in rice.

A loss-of-function *d14* mutant had a dwarf phenotype and a huge number of tillers (46 tillers per plant), whereas the gain-of-function *osmads57-1* mutant had a weak dwarf phenotype and a somewhat increased number of tillers (28 tillers per plant) (Fig. 5a,b and Supplementary Table S4). *d14osmads57-1*-double mutant plants (including both $D14^{-/-}OsMADS57^{-/-}$ and $D14^{-/-}OsMADS^{+/-}$) had a clearly elevated number of tillers (55 tillers per plant) and a dwarf phenotype, similar to the parental *d14* line, but dissimilar from the *osmads57-1* parent. *d14* is in a Shoikari (Shi) background, while *osmads57-1* is in the DJ background. WT plants of these backgrounds did not differ significantly in the tillering phenotype. As such, genetic analysis demonstrates that *OsMADS57* is functionally dependent on *D14*.

To explore the physiological correlation between SL signals and *OsMADS57*, the effects of SL on the transcription of *D14* (SL signalling) and *D27* (SL biosynthesis) were monitored in the *osmads57-1*. The expression level of untreated WT (DJ) was defined as the benchmark in qRT–PCR (Fig. 5c). The treatment of a synthetic SL, GR24, resulted in a decrease of *D27* transcription in both DJ and *osmads57-1*. This decrease was much more pronounced in *osmads57-1* than in DJ. Untreated *osmads57-1* showed a dramatically lower transcriptional level of *D27* compared with DJ, which may mimic the effect of GR24 on DJ. *D14* expression was induced by GR24 treatment in DJ and *osmads57-1*. In the non-treatment condition, the expression level of *D14* was obviously lower in *osmads57-1* than in DJ. Phenotypically, the outgrowth of axillary buds was repressed by GR24 treatment in DJ (Fig. 5d). In contrast, the repression was abolished in *osmads57-1*, which was similar to the SL-insensitive phenotype of the *d14* mutant[20,24]. Regardless of the treatment, the miROE line showed no axillary buds at the same developmental stage. They suggest that *OsMADS57* may be involved in SL signalling through *D14* in tillering of rice.

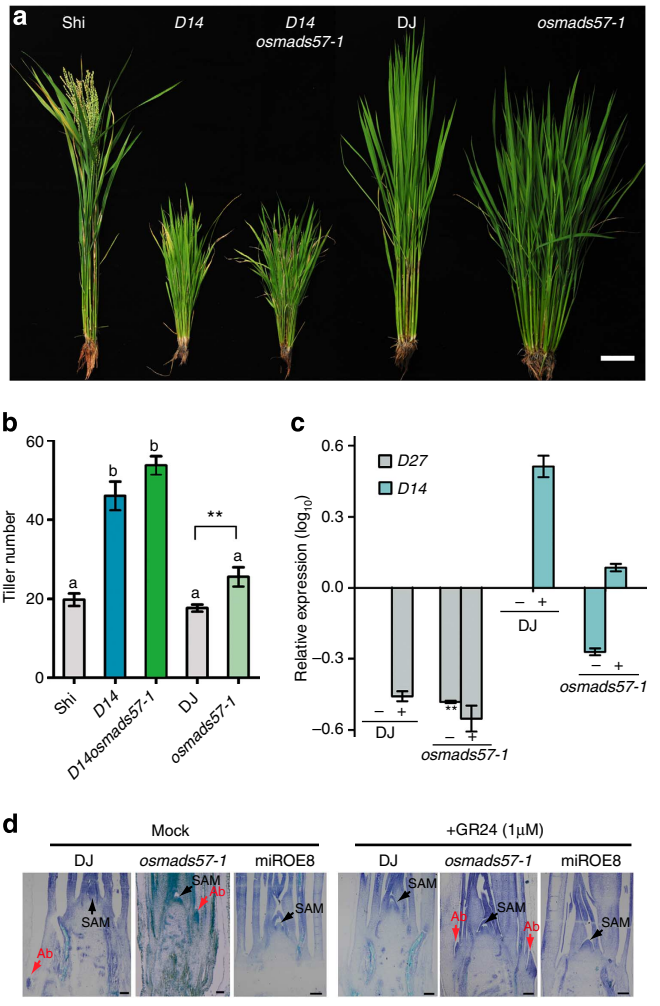

Figure 5 | Double mutant *d14osmads57-1* and response to GR24. (**a**,**b**) Tiller phenotypes and tiller number at heading stage. Scale bar, 10 cm. Different letters a and b represent significant differences among the lines (the least significant difference test, $P<0.05$). $^{**}P<0.01$ by Student's *t*-test. (**c**) *D27* and *D14* expression with (+) or without (−) 1 μM GR24. (**d**) Longitudinal sections of shoot apex treated with 1 μM GR24. Scale bars, 100 μm.

Transcription activity of OsMADS57 was affected by OsTB1. The rice mutant *tb1/fc1* has increased tillering, which is similar to *osmads57-1* (Fig. 1e–g) and *d14* (refs [12, 15]. Yeast two-hybrid (Y2H) assays showed that yeast cells cotransformed with constructs lacking its C-terminal region (OsMADS57N) could support growth in the selection medium and β-galactosidase staining (Fig. 6a). Thus, the truncated OsMADS57 lacking its intact C-terminal region (OsMADS57N) was sufficient to interact with OsMADS57. Y2H assays indicated that the interaction between OsTB1 and OsMADS57 appeared in yeast cells, and that OsTB1 was self-activated (Fig. 6b). Therefore, OsMADS57 was able to form a heterodimer with OsTB1.

Co-immunoprecipitation (Co-IP) tests revealed that the protein complexes pulled down by anti-c-Myc agarose were recognized by anti-Flag antibody in lines cotransformed with *cMyc-OsMADS57* and *Flag-OsMADS57*, or with *cMyc-OsTB1* and *Flag-OsMADS57* (Fig. 6c). Therefore, OsMADS57 could bind to itself and/or to OsTB1 *in planta*. Expression of *D14::LUC* was significantly repressed by OsMADS57 in protoplasts (Fig. 6d). By contrast, the extent of *D14::LUC* repression was reduced by cotransformation with *OsTB1*. When *OsMADS57* and a mutated version $OsTB1^{A159QWA162A163}$ were cotransformed, the activity pattern of *D14::LUC* was the same as *OsMADS57* alone. *OsTB1* alone did not obviously disturb the activity of *D14::LUC* in the system. A negative control, OsGRF4, did not affect *D14::LUC* activity (Fig. 6d). Therefore, OsMADS57 interacted directly with OsTB1, and this interaction could partially relieve the inhibitory effect of OsMADS57 on *D14* transcription (Fig. 6e).

Discussion

miR444a-dependent OsMADS57 regulates tiller development. In the model of MADS-box gene-mediated regulation of floral organogenesis and flowering, MADS transcription factors exert their function by forming homodimers or heterodimers, recognizing and binding the *cis*-element CArG boxes, and then regulating the expression of target genes[6,8,41]. The M-, I- and K-domains in MADS-box homeotic proteins lacking the

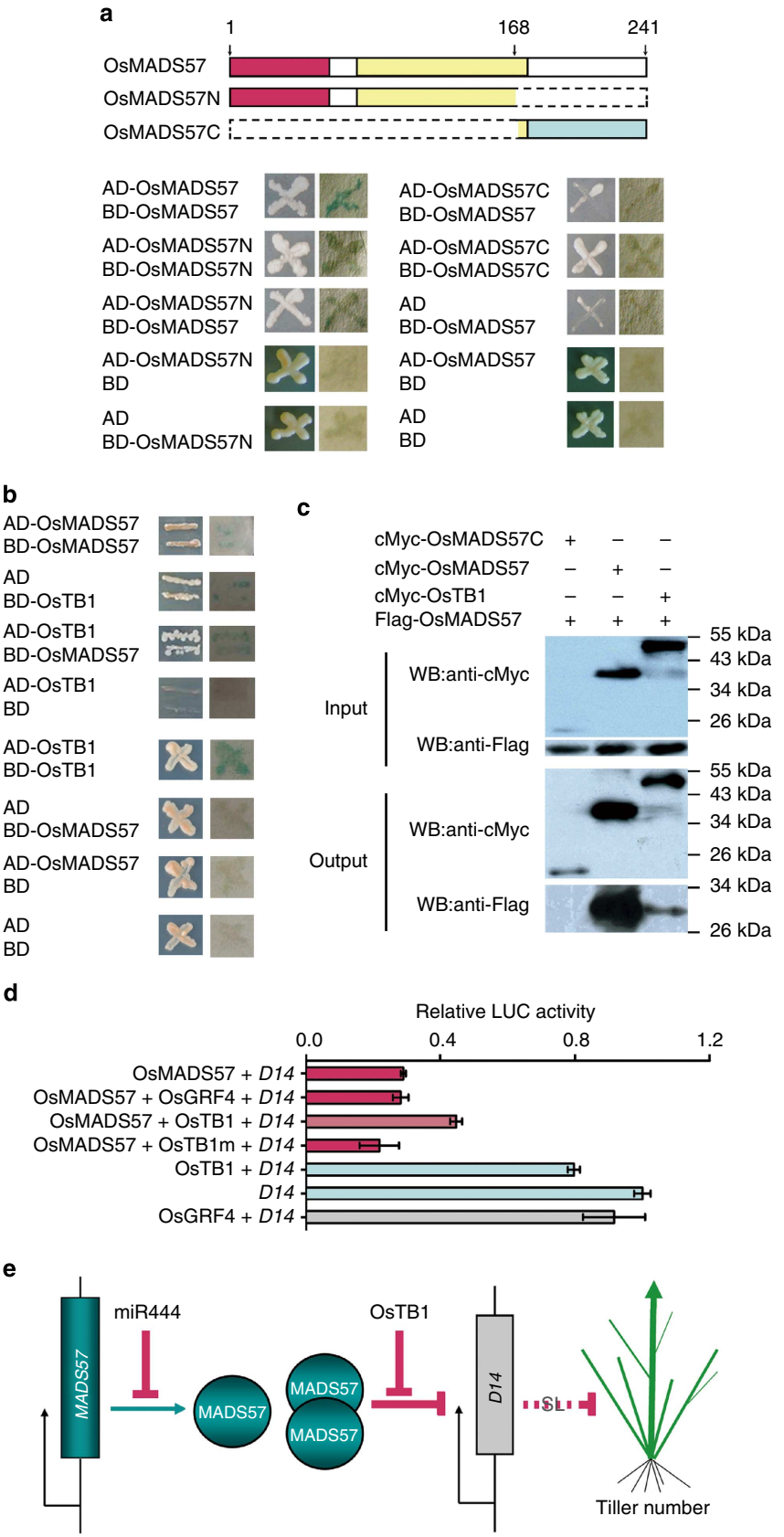

Figure 6 | OsMADS57 interaction with OsTB1. (**a**,**b**) Yeast two-hybrid assay. Diagrams represent the proteins. Yeast strains were grown on synthetic dropout medium lacking Trp, Leu, His and Ade, and stained for β-galactosidase activity. (**c**) Co-IP assay in Arabidopsis protoplasts. OsMADS57C, C-terminal 169–241 amino acids. (**d**) Effect of OsTB1 and OsTB1^{A159QWA162A163} (OsTB1m) on transcriptional regulation of *D14* via OsMADS57 in protoplasts. (**e**) Model of the OsMADS57-mediated network for control of tillering. WB, western blot.

C-terminal domain are sufficient for several MADS-box proteins to exert their functions in the investigated examples[4,42,43]. In the *AGL2*-like clade, the truncated proteins AGL1 and AGL2 lack the C-terminal domain, but can form homodimers and heterodimers and bind to the CArG boxes *in vitro*[4,42,43].

In this study, we demonstrated that the truncated OsMADS57 protein lacking an intact C-terminus was able to form dimers. The truncated *OsMADS57* gene acted as a gain-of-function gene for tiller development in the activation-tagged mutant *osmads57-1*. OsMADS57 also directly interacted with the TCP transcription factor OsTB1 at the protein level (Fig. 6). OsTB1 interaction with OsMADS57 reduced the negative regulation activity of OsMADS57 on *D14* expression, through which OsMADS57 affected tillering (Fig. 5a). The *OsMADS57* and *OsTB1* genes were expressed together at the shoot apical meristem and axillary buds. Our gain-of-function mutant *osmads57-1* and the loss-of-function mutant *ostb1/fc1* both had increased tillers, consistent with them acting in the same genetic pathway in rice (Figs 1 and 5)[12,15]. OsTB1 is a negative regulator controlling tiller outgrowth, whereas OsMADS57 is a positive regulator. Therefore, our data support the hypothesis that OsMADS57 can interact with OsTB1 to mediate transcriptional regulation of target genes, such as *D14*, and impact the outgrowth of axillary buds (Fig. 6e). This serves as another example of MADS and TCP family members directly functioning in vegetative organogenesis and development, as has been demonstrated for floral organogenesis in *Arabidopsis*[12–14].

Our data on the expression patterns of miR444a and *OsMADS57*, as well as the phenotypic analysis of the transgenic lines, support the prediction that miR444a directly targets *OsMADS57* to knockdown its transcript level and regulate tillering in rice (Fig. 2)[31,44]. Phenotypically, overexpression of miR444a resulted in decreased transcript levels of the *OsMADS57* gene and reduced tillering. As would be expected, this phenotype was similar to that of the *OsMADS57* antisense lines, but significantly different from that of the *OsMADS57*-overexpression lines, which showed increased tiller numbers (Fig. 2). As downregulation of *OsMADS57* expression mediated by miR444a suppressed tillering, it can be concluded that miR444a-dependent *OsMADS57* is involved in the regulation of tillering during rice development (Fig. 6e).

OsMADS57 directly repressed *D14* transcription to regulate tiller organogenesis. SL signalling and biosynthesis are involved in the regulation of branching in plants. DAD2, an orthologue of D14 in petunia, functions in SL perception and signalling. DAD2 binds to SL and interacts with the F-box protein PhMAX2A. The hydrolysis or binding of SL by DAD2 is required for DAD2 destabilization by the SCF (SKP1-CULLIN1-F-box) complex, which mediates signalling to regulate tillering[25]. *D27* and *D14* genes genetically function in the *MAX*/*RMS*/*D* pathway of SL biosynthesis[15,17,18,26,27]. It is possible that the function of *D14* in biosynthesis is likely a feedback effect of SL signalling. Analysis of the *d14osmads57-1*-double mutant indicated that *OsMADS57* was functionally dependent on *D14/D88* in rice tillering (Fig. 5). The *osmads57-1* mutant was insensitive to SL, similar to *d14*. The negative effect of SL on *D27* expression, as well as the abolished SL inhibition of outgrowth in *osmads57-1*, suggest that OsMADS57 is involved in *D14* function in the SL pathway to regulate tillering.

OsMADS57 interacted with OsTB1 and regulated tiller development in rice (Fig. 6). OsTB1/FC1 functions in the SL pathway to inhibit outgrowth of axillary buds, and is an integrator of multiple signalling pathways in rice[15,45]. The spatial expression pattern of *OsMADS57* is similar to *OsTB1/FC1* in axillary buds (Fig. 4)[15,45], and OsMADS57 physically interacted with OsTB1/FC1 (Fig. 6). OsMADS57 may be involved in balancing the *D14*-mediated SL signalling pathway through its protein interaction with OsTB1/FC1 (ref. 15). The gain-of-function mutants *osmads57-1* and *ostb1/fc1*, as well as the loss-of-function *mutant d14* were insensitive to SL treatment (Fig. 5)[20,21,24,40]. At the protein level, OsMADS57 physically interacted with OsTB1/FC1 to regulate *D14* expression, and requires the $V_{159}XXL_{162}L_{163}$ motif in OsTB1 (Fig.6)[15,46]. The VXXLL motif is a signature sequence in the transcriptional coactivators and mediates binding to liganded nuclear receptors in animal cells[47]. Consistently, OsTB1/FC1 functions as a negative regulator of the SL signalling pathway[15]. It is possible that *OsMADS57* is required for the SL signalling pathway to inhibit bud growth. *D14* expression was downregulated in the *osmads57-1* mutant. The SL-mediated induction of *D14* expression remains strong in *osmads57-1* (>2-fold), although it was less than that in WT. This suggests that SL-induced *D14* expression is counterbalanced by the repression of OsMADS57 on transcription. Together, our data indicate that OsMADS57, along with OsTB1, regulates the expression of *D14* (Fig. 6e).

MADS-box transcription factors recognize *cis*-element CArG boxes. Our data from the binding and transcription assays suggest that OsMADS57 interacts with its preferred CArG-box motif [C(A/T)TTAAAAAG] in the promoter of the *D14* gene to suppress expression. The transcriptional repression activity of OsMADS57 on *D14* was reduced by its protein interaction with OsTB1 as a heterodimer (Fig. 6). In the transgenic lines, as well as the *osmads57-1* mutant, *D14* expression was negatively regulated by OsMADS57 *in planta* (Fig. 4g). Thus, the MADS and TCP complexes with homodimer and/or heterodimer may be involved in regulating branching[48]. Opposite tillering phenotypes were observed between the loss-of-function *ostb1* and the *OsMADS57*-knockdown lines of overexpressing miR444a or antisense *OsMADS57*, whereas similar phenotypes were found in *ostb1* and the gain-of-function *osmads57-1*. *D14* expression was reduced at the axillary buds in *osmads57-1* (Figs 3f and 4g), which is consistent with the phenotype of the *d14* mutant[20,24]. Together, this suggests that the interactions of MADS-box (OsMADS57) and TCP (OsTB1) transcription factors result in a dynamic balance of the target gene expression during tillering. This finding enhances our understanding of the function of this conserved MADS-box protein and its mediating network involving well-known genes, such as *OsTB1* and *D14*, that are known to control tillering[15,20].

In summary, tillering in rice involves a miRNA/MADS/TCP/D14 (miMTD) regulation module or network, in which OsMADS57, modulated by its interaction with OsTB1, directly represses *D14* expression, which is in turn involved in SL perception and signalling[25]. Furthermore, the *OsMADS57* gene is targeted and regulated negatively by miR444a. The discovery of such a miMTD regulation mechanism for tillering has great potential application for use in efforts to increase yields through rice molecular breeding programs.

Methods

Plant materials. The T-DNA insertion mutant line PFG_3A-05432.L (*osmads57-1*) in an *Oryza sativa* ssp *japonica* cv Dongjin background was obtained from RiceGE, the Rice Functional Genomics Express Database, in Pohang city, Korea. The *d14/d88* mutant was a gift from Qian's lab, China Insititute of Rice Biology. All transgenic lines were developed in the genetic background of *O. sativa* ssp *japonica* cv Zhonghua10 (ZH10). Rice plants were grown in a temperature-controlled greenhouse with 30 °C/25 °C day/night cycles. The analysis of tiller numbers used materials from ten plants from each line. Developing axillary buds from *osmads57-1* and Dongjin 30 DAG were used in the microarray experiments.

Transformation of rice plants. Genetic transformation of rice plants was performed using *Agrobacterium*-mediated methods. Full-length cDNA of the

OsMADS57 gene in a sense orientation was used for the overexpression construct. The *OsMADS57* gene in an antisense orientation was used for the antisense construct. The constructed vectors were transformed with the use of *Agrobacterium tumefaciens* strain EHA105. All primers used in the study are presented in Supplementary Table S5.

Quantitative RT–PCR. Total RNA was extracted using a TRIzol RNA extraction kit (Invitrogen) and treated with RNase-free DNase I (MBI Fermentas). RNA was used to synthesize cDNA using AMV Reverse Transcriptase (Promega). Quantitative RT–PCR was performed on a Mx3000P instrument (Stratagene) with SYBR Green Real-time PCR Master Mix (Toyobo) according to the manufacturer's instructions. Gene expression was normalized to that of ACTIN. miRNA levels were normalized to 5.8S rRNA levels by qRT–PCR. The relative expression level ($\log_{10}$) in the WT ZH10 line was defined as 0. Experiments included three technical replicates and at least three biological replicates. Values represent means ± s.e. of three technical replicates. Primers used for qRT–PCR are presented in Supplementary Table S5.

***In situ* hybridization**. *In situ* hybridization was performed as described previously[49]. Digoxigenin-labelled hybrid probes were transcribed *in vitro* from cDNA of *OsMADS57*, *ACTIN* and *D14* with gene-specific primers (Supplementary Table S5). SAM and axillary buds were used for hybridization assays. Slides were photographed under a microscope (Zeiss).

Yeast one-hybrid assays. Yeast one-hybrid assays were used to check binding of OsMADS57 to *D14*[50]. cDNA encoding full-length OsMADS57 and OsMADS57N (amino acids 1–168) were inserted into pGAD424 to generate pGAD424-OsMADS57 and pGAD424-OsMADS57N, respectively. The effectors contained the GAL4-activation domain. To generate the *D14p-Pcyc1::LacZ* reporter plasmid, a *D14* promoter was amplified with the primers D14pEcoRIF and D14XhoIR. These constructs were transformed into the *Saccharomyces cerevisiae* strain EGY48. Transformed yeast was selected on synthetic complete medium lacking Ura and Leu[50].

Yeast two-hybrid assays. The cDNAs for OsMADS57, OsMADS57N, OsMADS57C, OsTB1 and OsTB1^{A159QWA162A163} were cloned into the pGADT7 and pGBKT7 (Stratagene) vectors. These constructs were transformed into *S. cerevisiae* strain AH109. Individual colonies of transformants were screened by growing on medium lacking Leu, Trp and His. Recovered clones were transferred onto a filter paper and then assayed for LacZ activity.

Protoplast transformation and transient expression assays. The transcription activity assay was carried out in the transient-transformed protoplast. The DNA-binding domain (BD) from GAL4 was used in the system[34]. The GAL4 BD–OsMADS57 fusion protein can bind to the GAL4 DNA-binding sites of the GUS reporter. Two known proteins HOS15, a transcription suppressor, and ARF5M, an activator, were used as the controls. The *GUS* reporter containing four upstream *GAL4* DNA-binding sites (*GAL4* (4X)-D1-3(4X)-*GUS*) and the luciferase (*LUC*) reporter were cotransformed with *GAL4 BD–OsMADS57* into Arabidopsis protoplasts. The *LUC* reporter carrying the luciferase gene under control of CaMV 35S promoter was used as the internal control to normalize the data for eliminating variations in the experiment.

For the specific binding and repressing activity to *D14* promoter assay, OsMADS57 and its mutated forms were used in the system[50]. The cDNAs for full-length *OsMADS57*, *OsMADS57N*, and *OsMADS57F* were fused into the pBI221 vector driven by the 35S promoter to generate pBI221-OsMADS57, pBI221-OsMADS57N and pBI221-OsMADS57F, respectively. To generate the *D14:LUC* reporter gene, the *D14* promoter was amplified. The plasmid carrying the *GUS* gene under the control of the 35S promoter was used as a normalization control. Values represent means ± s.e. of three technical replicates. Cotransformation of *OsMADS57* and *OsTB1* was done for identifying effect of OsTB1 in the transient assay. As a control, OsTB1^{V159QWL162L163} was replaced with OsTB1^{A159QWA162A163} to disturb its interaction with OsMADS57 (ref. 47).

Electrophoretic mobility shift assays. EMSAs were performed to identify the binding activity of OsMADS57 to the potential motifs[51]. Oligonucleotides complementary to different motifs of the *D14* promoter were synthesized and labelled using a Biotin 3′ End DNA Labeling Kit (Pierce). For supershift assays, anti-GST antiserum (Sigma-Aldrich) was added to the reaction.

Chromatin immunoprecipitation assays. To confirm the binding activity of OsMADS57 to *D14 in vivo*, chromatin immunoprecipitation (ChIP) assay was carried out using the root-dislodged 2-week-old seedlings[52]. Purified anti-OsMADS57 polyclonal antibody (BGI, Beijing) was used for IP. As negative controls, an agarose/Salmon sperm DNA (Millipore) with the preimmune serum was used. The DNA products of IP were analysed by qRT–PCR. The enrichment was calculated as the ratio of *osmads57-1* to DJ (I). Data are mean ± s.d. of three independent experiments. The primers used in the ChIP assays are listed in Supplementary Table S5.

Co-IP assays. To validate the proteins interaction of OsMADS57 and OsTB1 *in vivo*, Co-IP assay approach was used[53]. The cDNAs for *OsMADS57*, *OsMADS57C* and *OsTB1* were amplified using the primers MSNCFBamHI and MSNCRKpnI, OsMADS57BamHIF and OsMADS57KpnIR, and OsTB1BamHI sense and OsTB1KpnI antisense, respectively. Amplified cDNAs were inserted into pRT107-6XMyc or pRT105-3XFlag[53] between BamHI and KpnI sites to generate the four expression vectors *2 × 35S::6XMyc-OsMADS57C*, *2 × 35S::6XMyc-OsMADS57*, *2 × 35S::3XFag-OsMADS57* and *2 × 35S::6XMyc-OsTB1*. Protoplasts from *Arabidopsis thaliana* (Col-0) were isolated and transformed using a polyethylene glycol-mediated technique[54]. Both anti-c-Myc and anti-Flag antibodies (Sigma-Aldrich) were used. The crude protein extract was used as input and the products pulled down by the anti-c-Myc agarose conjugate were used as output. All primers used in the study are presented in Supplementary Table S5.

Histological analyses. Seedlings were treated with 1 μM GR24 in Kimura B nutrient solution[55] for 8 days. Tissues of SAM and axillary buds from 15-day-old plants were fixed and sectioned into 7-μm sections and stained with toluidine blue or fuschin red for light microscopic analysis (Zeiss).

Subcellular localization of fusion protein in protoplast. A transient expression vector, 35S:GFP-OsMADS57, was constructed. For protoplast transformation, the released protoplast cells from leaf sheaths of 10-day-old etiolated rice seedlings were isolated and transformed via the polyethylene glycol (PEG 4000) method[56]. At the same time, Hoechst 33342 was used to stain the nucleic acids that were then visualized at an excitation wavelength of 405 nm.

Phylogenetic analysis. The phylogenetic analysis of 20 MADS-box protein sequences from Arabidopsis, rice, maize and wheat was performed using MEGA 4.0, with default settings and the neighbour-joining method. Bootstrap values (%) of 2,000 replicates are shown at the branching points.

References

1. Dreni, L. *et al.* Functional analysis of all AGAMOUS subfamily members in rice reveals their roles in reproductive organ identity determination and meristem determinacy. *Plant Cell* **23,** 2850–2863 (2011).
2. Li, H. *et al.* Rice MADS6 interacts with the floral homeotic genes SUPERWOMAN1, MADS3, MADS58, MADS13, and DROOPING LEAF in specifying floral organ identities and meristem fate. *Plant Cell* **23,** 2536–2552 (2011).
3. Lim, J., Moon, Y. H., An, G. & Jang, S. K. Two rice MADS domain proteins interact with OsMADS1. *Plant Mol. Biol.* **44,** 513–527 (2000).
4. Huang, H. *et al.* DNA binding properties of two Arabidopsis MADS domain proteins: binding consensus and dimer formation. *Plant Cell* **8,** 81–94 (1996).
5. Cui, R. *et al.* Functional conservation and diversification of class E floral homeotic genes in rice (*Oryza sativa*). *Plant J.* **61,** 767–781 (2010).
6. Tang, W. & Perry, S. E. Binding site selection for the plant MADS domain protein AGL15: an *in vitro* and *in vivo* study. *J. Biol. Chem.* **278,** 28154–28159 (2003).
7. Riechmann, J. L., Krizek, B. A. & Meyerowitz, E. M. Dimerization specificity of Arabidopsis MADS domain homeotic proteins APETALA1, APETALA3, PISTILLATA, and AGAMOUS. *Proc. Natl Acad. Sci. USA* **93,** 4793–4798 (1996).
8. Matias-Hernandez, L. *et al.* VERDANDI is a direct target of the MADS domain ovule identity complex and affects embryo sac differentiation in Arabidopsis. *Plant Cell* **22,** 1702–1715 (2010).
9. Arora, R. *et al.* MADS-box gene family in rice: genome-wide identification, organization and expression profiling during reproductive development and stress. *BMC Genomics* **8,** 242 (2007).
10. Tapia-Lopez, R. *et al.* An AGAMOUS-related MADS-box gene, XAL1 (AGL12), regulates root meristem cell proliferation and flowering transition in Arabidopsis. *Plant Physiol.* **146,** 1182–1192 (2008).
11. Clark, R. M., Linton, E., Messing, J. & Doebley, J. F. Pattern of diversity in the genomic region near the maize domestication gene tb1. *Proc. Natl Acad. Sci. USA* **101,** 700–707 (2004).
12. Takeda, T. *et al.* The OsTB1 gene negatively regulates lateral branching in rice. *Plant J.* **33,** 513–520 (2003).
13. Aguilar-Martinez, J. A., Poza-Carrion, C. & Cubas, P. Arabidopsis BRANCHED1 acts as an integrator of branching signals within axillary buds. *Plant Cell* **19,** 458–472 (2007).
14. Barkoulas, M., Galinha, C., Grigg, S. P. & Tsiantis, M. From genes to shape: regulatory interactions in leaf development. *Curr. Opin. Plant Biol.* **10,** 660–666 (2007).

15. Minakuchi, K. *et al.* FINE CULM1 (FC1) works downstream of strigolactones to inhibit the outgrowth of axillary buds in rice. *Plant Cell Physiol.* **51,** 1127–1135 (2010).
16. Stirnberg, P., van de Sande, K. & Leyser, H. M. O. MAX1 and MAX2 control shoot lateral branching in Arabidopsis. *Development* **129,** 1131–1141 (2002).
17. Sorefan, K. *et al.* MAX4 and RMS1 are orthologous dioxygenase-like genes that regulate shoot branching in Arabidopsis and pea. *Genes Dev.* **17,** 1469–1474 (2003).
18. Arite, T. *et al.* DWARF10, an RMS1/MAX4/DAD1 ortholog, controls lateral bud outgrowth in rice. *Plant J.* **51,** 1019–1029 (2007).
19. Lin, H. *et al.* DWARF27, an iron-containing protein required for the biosynthesis of strigolactones, regulates rice tiller bud outgrowth. *Plant Cell* **21,** 1512–1525 (2009).
20. Arite, T. *et al.* d14, a strigolactone-insensitive mutant of rice, shows an accelerated outgrowth of tillers. *Plant Cell Physiol.* **50,** 1416–1424 (2009).
21. Li, X. *et al.* Control of tillering in rice. *Nature* **422,** 618–621 (2003).
22. Lin, Q. *et al.* Rice APC/C(TE) controls tillering by mediating the degradation of MONOCULM 1. *Nat. Commun.* **3,** 752 (2012).
23. Xu, C. *et al.* Degradation of MONOCULM 1 by APC/C(TAD1) regulates rice tillering. *Nat. Commun.* **3,** 750 (2012).
24. Gao, Z. *et al.* Dwarf 88, a novel putative esterase gene affecting architecture of rice plant. *Plant Mol. Biol.* **71,** 265–276 (2009).
25. Hamiaux, C. *et al.* DAD2 is an alpha/beta hydrolase likely to be involved in the perception of the plant branching hormone, strigolactone. *Curr. Biol.* **22,** 1–5 (2012).
26. Booker, J. *et al.* MAX1 encodes a cytochrome P450 family member that acts downstream of MAX3/4 to produce a carotenoid-derived branch-inhibiting hormone. *Dev. Cell* **8,** 443–449 (2005).
27. Zou, J. *et al.* The rice HIGH-TILLERING DWARF1 encoding an ortholog of Arabidopsis MAX3 is required for negative regulation of the outgrowth of axillary buds. *Plant J.* **48,** 687–698 (2006).
28. Liu, W. *et al.* Strigolactone biosynthesis in medicago truncatula and rice requires the symbiotic GRAS-type transcription factors NSP1 and NSP2. *Plant Cell* **23,** 3853–3865 (2011).
29. Becker, A. & Theissen, G. The major clades of MADS-box genes and their role in the development and evolution of flowering plants. *Mol. Phylogenet. Evol.* **29,** 464–489 (2003).
30. Jeong, D. H. *et al.* T-DNA insertional mutagenesis for activation tagging in rice. *Plant Physiol.* **130,** 1636–1644 (2002).
31. Sunkar, R., Girke, T., Jain, P. K. & Zhu, J. K. Cloning and characterization of microRNAs from rice. *Plant Cell* **17,** 1397–1411 (2005).
32. Hanada, K., Zhang, X., Borevitz, J. O., Li, W. H. & Shiu, S. H. A large number of novel coding small open reading frames in the intergenic regions of the *Arabidopsis thaliana* genome are transcribed and/or under purifying selection. *Genome Res.* **17,** 632–640 (2007).
33. Hruz, T. *et al.* Genevestigator v3: a reference expression database for the meta-analysis of transcriptomes. *Adv. Bioinformatics* **2008,** 420747 (2008).
34. Zhu, J. *et al.* Involvement of Arabidopsis HOS15 in histone deacetylation and cold tolerance. *Proc. Natl Acad. Sci. USA* **105,** 4945–4950 (2008).
35. Lo, S. F. *et al.* A novel class of gibberellin 2-oxidases control semidwarfism, tillering, and root development in rice. *Plant Cell* **20,** 2603–2618 (2008).
36. Tong, H. *et al.* DWARF AND LOW-TILLERING, a new member of the GRAS family, plays positive roles in brassinosteroid signaling in rice. *Plant J.* **58,** 803–816 (2009).
37. Ishikawa, S. *et al.* Suppression of tiller bud activity in tillering dwarf mutants of rice. *Plant Cell Physiol.* **46,** 79–86 (2005).
38. Tong, H. *et al.* DWARF AND LOW-TILLERING acts as a direct downstream target of a GSK3/SHAGGY-like kinase to mediate brassinosteroid responses in rice. *Plant Cell* **24,** 2562–2577 (2012).
39. de Folter, S. & Angenent, G. C. Trans meets cis in MADS science. *Trends Plant Sci.* **11,** 224–231 (2006).
40. Liu, W. *et al.* Identification and characterization of HTD2: a novel gene negatively regulating tiller bud outgrowth in rice. *Planta* **230,** 649–658 (2009).
41. Lee, J., Oh, M., Park, H. & Lee, I. SOC1 translocated to the nucleus by interaction with AGL24 directly regulates leafy. *Plant J.* **55,** 832–843 (2008).
42. Piwarzyk, E., Yang, Y. & Jack, T. Conserved C-terminal motifs of the Arabidopsis proteins APETALA3 and PISTILLATA are dispensable for floral organ identity function. *Plant Physiol.* **145,** 1495–1505 (2007).
43. Su, K. M. *et al.* The MIK region rather than the C-terminal domain of AP3-like class B floral homeotic proteins determines functional specificity in the development and evolution of petals. *New Phytol.* **178,** 544–558 (2008).
44. Kutter, C., Schob, H., Stadler, M., Meins, Jr F. & Si-Ammour, A. MicroRNA-mediated regulation of stomatal development in Arabidopsis. *Plant Cell* **19,** 2417–2429 (2007).
45. Koyama, T., Furutani, M., Tasaka, M. & Ohme-Takagi, M. TCP transcription factors control the morphology of shoot lateral organs via negative regulation of the expression of boundary-specific genes in Arabidopsis. *Plant Cell* **19,** 473–484 (2007).
46. Cubas, P., Lauter, N., Doebley, J. & Coen, E. The TCP domain: a motif found in proteins regulating plant growth and development. *Plant J.* **18,** 215–222 (1999).
47. Heery, D. M. *et al.* A signature motif in transcriptional co-activators mediates binding to nuclear receptors. *Nature* **387,** 733–736 (1997).
48. Immink, R. G., Kaufmann, K. & Angenent, G. C. The 'ABC' of MADS domain protein behaviour and interactions. *Semin. Cell Dev. Biol.* **21,** 87–93 (2010).
49. Xu, Y. Y. *et al.* Activation of the WUS gene induces ectopic initiation of floral meristems on mature stem surface in *Arabidopsis thaliana*. *Plant Mol. Biol.* **57,** 773–784 (2005).
50. Lin, R. *et al.* Transposase-derived transcription factors regulate light signaling in Arabidopsis. *Science* **318,** 1302–1305 (2007).
51. Ma, Q. *et al.* Enhanced tolerance to chilling stress in OsMYB3R-2 transgenic rice is mediated by alteration in cell cycle and ectopic expression of stress genes. *Plant Physiol.* **150,** 244–256 (2009).
52. He, J. X. *et al.* BZR1 is a transcriptional repressor with dual roles in brassinosteroid homeostasis and growth responses. *Science* **307,** 1634–1638 (2005).
53. Zhao, J. *et al.* SAD2, an importin-like protein, is required for UV-B response in Arabidopsis by mediating MYB4 nuclear trafficking. *Plant Cell* **19,** 3805–3818 (2007).
54. Yoo, S. D., Cho, Y. H. & Sheen, J. Arabidopsis mesophyll protoplasts: a versatile cell system for transient gene expression analysis. *Nat. Protoc.* **2,** 1565–1572 (2007).
55. Kato-Noguchi, H. & Ino, T. Possible involvement of momilactone B in rice allelopathy. *J. Plant Physiol.* **162,** 718–721 (2005).
56. Bart, R., Chern, M., Park, C. J., Bartley, L. & Ronald, P. C. A novel system for gene silencing using siRNAs in rice leaf and stem-derived protoplasts. *Plant Methods* **2,** 13 (2006).

Acknowledgements

We thank Dr Yan Guo for assisting with the Co-IP analysis, Dr Ray A. Bressan (Purdue University) for providing the transcription repression system, Dr Rongcheng Lin for assisting with the yeast one-hybrid and luciferase systems, Dr Jingbo Jin for providing the 326-nGFP plasmid, Dr Lijia Qu for supplying GR24 and Ms Rongxi Jiang for assisting with gene transformation, as well as Jun Xiao for his help on the project. This work was funded by grants from the National Nature Science Foundation of China (31070248; 31121065), and the state Hi-Tech Research and Development program of China (2012AA10A301), and the Major Basic Research Program (2011CB100204).

Author contributions

S.Y.G. performed the experiments, analysed data and wrote the paper; Y.Y.X. designed experiments, analysed data and wrote the paper; Z.W.M., C.Z., Y.M., H.H.L. and Q.R.Z. performed a part of experiments and data analysis; Z.M. designed experiments and analysed data; and K.C. designed the experiments, analysed data and wrote the paper.

Additional information

Supplementary Information accompanies this paper at http://www.nature.com/naturecommunications

Competing financial interests: The authors declare no competing financial interests.

Reprints and permission information is available online at http://npg.nature.com/reprintsandpermissions/

How to cite this article: Guo, S. *et al.* The interaction between OsMADS57 and OsTB1 modulates rice tillering via *DWARF14*. *Nat. Commun.* 4:1566 doi: 10.1038/ncomms2542 (2013).